

The Changes in Extreme Precipitation over Malaysia During Boreal Winter

*Bokri Noor Amalina*¹ and *Salimun Ester*^{1*}

¹ Department of Earth Sciences and Environment, Faculty Science and Technology, Universiti Kebangsaan Malaysia, 43600 Bangi, Selangor Malaysia

Abstract. Climate change is altering the Earth's atmospheric and oceanic conditions, leading to increased frequency and intensity of extreme weather patterns. This study evaluates the ability of three High-Resolution Model Intercomparison Project (HighResMIP) CMIP6 models, CMCC-CM2-VHR4, MRI-AGCM3-2-S, and FGOALS-F3-H to simulate extreme precipitation events during boreal winter over Malaysia. Three extreme indices, Consecutive Wet Days (CWD), Simple Precipitation Intensity Index (SDII) and Total Precipitation (PRCPTOT) from the Expert Team on Sector-Specific Climate Indices (ET-SCI) have been utilized for analysis. Future projections of extreme rainfall are based on the most accurate model identified from this evaluation. Statistical methods including the Taylor diagram and significance test are employed in the analysis. Results indicate that the MRI-AGCM3-2-S model exhibits superior capability in simulating all three extreme indices over the study region. This information provides valuable insights for local authorities to strategise their mitigation and adaptation plans at the local scale.

1 Introduction

Extreme events like flash floods, heatwaves, and landslides not only incur economic losses but also result in considerable loss of life. In Malaysia, the condition is wetter during boreal winter season, December-January-February (DJF) due to the Asian-Australian monsoon [1-3]. The most recent catastrophic disaster to strike Malaysia has cost the nation RM 6.1 billion, which occurred in January 2022 [4]. According to the latest report from the Department of Statistics Malaysia (DOSM), flooding in 2023 alone resulted in a loss of RM 0.8 billion (Bernama 2024).

HighResMIP is the first of its kind, which utilizes a multi-model General Circulation Model (GCM) approach to systematically study the implications of horizontal resolution [5]. High-resolution GCMs with the latest CMIP6 are particularly suited for simulating local-

* Corresponding author: ester@ukm.edu.my

scale rainfall patterns due to their enhanced ability to capture finer details of atmospheric processes [6].

The Maritime Continent is projected to increase in extreme precipitation by approximately 30% under RCP 4.5 and 60% under RCP 8.5, particularly in index Consecutive Dry Days (CDD) using 25 km resolution of CORDEX output [7]. It also projected a decrease in PRCPTOT during June-July-August (JJA) and September-October-November (SON). Due to the lack of information on extreme precipitation analysis over this region including Malaysia, this research is designed to bridge the gaps. The goals of this study are to evaluate three HighResMIP CMIP6 models in simulating extreme precipitation over Malaysia during the boreal winter season. The best model will be used to project future extreme precipitation. The future changes under scenario SSP5-8.5 will be evaluated to understand the trend of extreme precipitation patterns over this country.

2 Methodology

The study location is Malaysia which consists of Peninsular and East Malaysia. Located in Southeast Asia, this region is influenced by the Asian-Australian monsoon during boreal winter. Three HighResMIP CMIP6 global climate models (GCMs) with approximately 25 km resolution: specifically, CMCC-CM2-VHR4, FGOALS-f3-H, and MRI-AGCM3-2-S were employed. The study utilized a baseline period from 1982 to 2014, and the projection periods extended from 2015 to 2050, under the SSP5-8.5 scenario. For observational data, gridded daily datasets from the Climate Hazards Group InfraRed Precipitation with Station data (CHIRPS), which also have a 25 km resolution, were used.

Three indices from the Expert Team on Sector-Specific Climate Indices (ET-SCI) were employed for calculating extreme precipitation. The performance of the models was statistically summarized in terms of correlation, standard deviation, and root mean square error, with the results displayed in a Taylor diagram. The study analyzed changes in extreme precipitation characteristics by comparing the outputs from the baseline and projection periods. A significance test was applied to the changes in all extreme indices, with a 95% confidence level.

2.1 Rainfall extreme indices

Three extreme indices from ET-SCI were chosen because they calculate the amount of rainfall that suits the situation in Malaysia, which receives a high amount of rain during the boreal winter season (DJF). The changes in these climate extremes indices could have significant societal impacts [8, 9]. Table 1 lists the extreme precipitation indices from ET-SCI that will be utilised in this study.

Table 1. List of extreme precipitation from ET-SCI used in this study.

| Name | Index | Description | Unit |
|--|---------|---|----------|
| Consecutive Wet Days | CWD | Maximum number of consecutive days where $rr \geq 1$ mm | Days |
| Annual total precipitation on wet days | PRCPTOT | Total wet day precipitation | mm |
| Simple Precipitation Intensity Index | SDII | Simple daily intensity | mm/ days |

2.2 Observation and model data

An observation dataset of rainfall is used from CHIRPS which has a resolution of 25 km. Table 2 lists the model of HighResMIP-CMIP6 used in the research. Every model has a corresponding resolution as shown in the table.

Table 2. Institute and model names of the HighResMIP- CMIP6 GCMs used.

| Model Name | Institute | Shortform | Resolution |
|---------------|--|-----------|---------------|
| CMCC-CM2-VHR4 | Centro Euro – Meiterraneo sui Cambiamenti Climatici | CMCC | 0.31° x 0.31° |
| MRI-AGCM3-2-S | Meteorological Research Institute (Japan) | MRI | 0.19° x 0.19° |
| FGOALS-f3-H | Chinese Academy of Sciences Flexible Global Ocean-Atmosphere-Land System Model | FGOALS | 0.25° x 0.25° |

2.3 Statistical analysis on the spatial distribution of rainfall

The models are validated using the Taylor diagram statistic values [10], which include correlation, root mean square error, and standard deviation. It compares the climatology of climate indices for the models and observations.

3 Results and Discussion

3.1 Historical rainfall extreme during boreal winter

Based on the observation and three HighResMIP models (FGOALS, MRI, and CMCC), the spatial distributions of extreme indices are portrayed. Figure 1 shows the spatial distribution of CWD over Malaysia during boreal winter (DJF). The whole of Malaysia encountered wet condition during DJF (Figure 1a). FGOALS model simulates few locations receiving high numbers of wet days over the northern part of both Peninsular and East Malaysia (Figure 1b). MRI model simulate more wet days over the East Malaysia and most of coastal part of

Peninsular (Figure 1c), however the CMCC model's prediction (Figure 1d) disagrees with the observation.

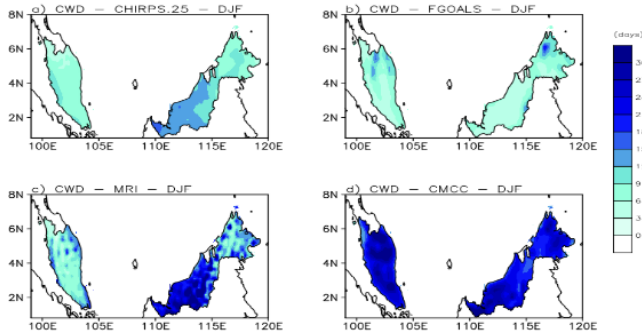


Figure 1. The climatology pattern of the spatial distribution of Consecutive Wet Days (CWD) from CHIRPS, FGOALS, MRI and CMCC during DJF. The index represents extreme precipitation obtained for the period from 1982 to 2014.

A statistical comparison between the models and the simulation of observation is shown in the Taylor diagram. The result from Figure 1 is supported by statistical analysis of CWD (Figure 2). Model MRI revealed the highest correlation, which was followed by CMCC and FGOALS. However, compared to other models, FGOALS has a lower RMSE which is most likely a result of less simulation on rainy days over the state of Sarawak (Figure 1c).

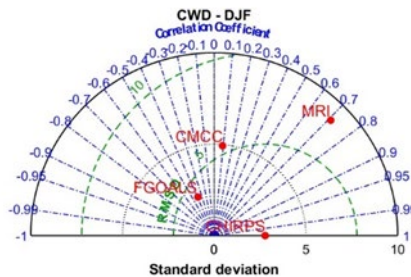


Figure 2. Taylor diagram of the spatial distribution of the simulated CWD. The spatial correlation between the models and observations is displayed on the azimuthal axis, whilst the x-axis indicates the standard deviation. The green dashed line represents the root mean square error (RMSE).

Next, the research area's total annual precipitation (PRCPTOT) regional distribution is depicted in Figure 3. Based on the pattern, Malaysia receives up to 1300 mm of rain throughout this season, which is heavy for the country as observed by the observation datasets (Figure 3a). All three models show their ability to simulate the PRCPTOT index closely to the observation (Figure 3b, c, d). This aligns with research by Liang et al. (2022) that found that during the Northeast monsoon season November-December-January-February (NDJF), the Peninsular receives drastically greater precipitation, especially on the east coast.

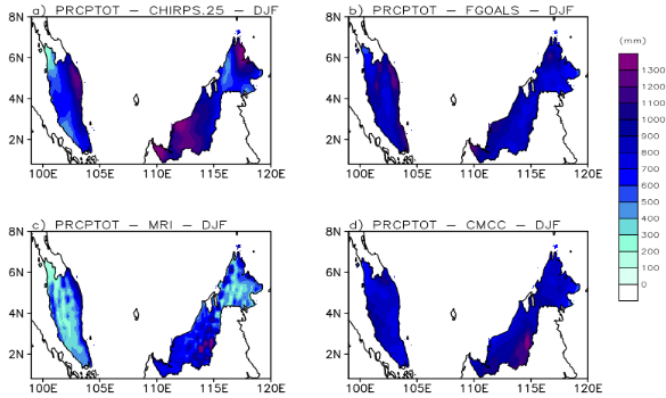


Figure 3. The climatology pattern of the spatial distribution of total annual precipitation (PRCPTOT) from CHIRPS, FGOALS, MRI and CMCC during DJF. The index represents the extreme precipitation obtained for the period from 1982 to 2014.

Statistical analysis of PRCPTOT (Figure 4) agreed that model MRI has a high correlation with the observation. Although not many differences between FGOALS and CMCC in terms of RMSE and standard deviation, model MRI is more reliable for simulating index PRCPTOT over Malaysia during DJF.

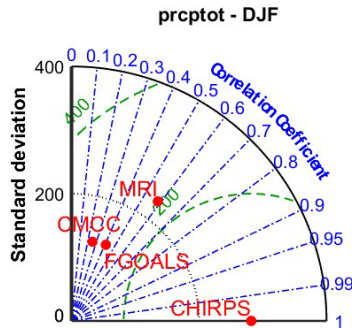


Figure 4. Taylor diagram of the spatial distribution of the simulated PRCPTOT. The spatial correlation between the models and observations is displayed on the azimuthal axis, whilst the x-axis indicates the standard deviation. The green dash line represents root mean square error (RMSE).

Figure 5 illustrates the simple daily intensity of rainfall (SDII) during DJF. The east coast of Peninsular and most of East Malaysia receive high rainfall during this season due to northeast monsoon (Figure 3a, b).

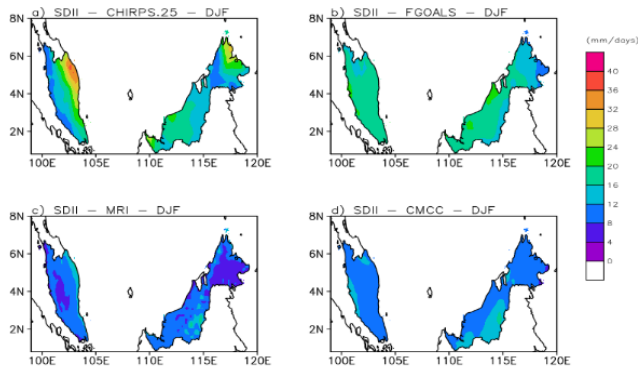


Figure 5. The climatology pattern of the spatial distribution of the simple daily intensity of rainfall (SDII) from CHIRPS, FGOALS, MRI and CMCC during DJF. The index represents the extreme precipitation obtained for the period from 1982 to 2014.

Results from statistical analysis agree that model MRI is located close to the observation (Figure 4). It has a high correlation and low RMSE compared to the other two models, FGOALS and CMCC.

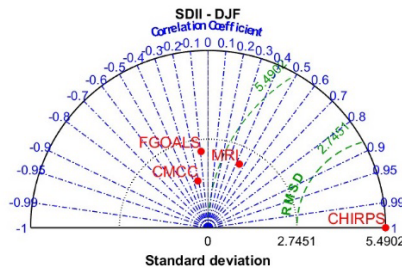


Figure 6. Taylor diagram of the spatial distribution of the simulated PRCPTOT. The spatial correlation between the models and observations is displayed on the azimuthal axis, whilst the x-axis indicates the standard deviation. The green dash line represents the root mean square error (RMSE).

Table 3 shows the summary of model performance in simulating extreme precipitation indices during boreal winter, DJF over Malaysia. Model MRI-AGCM3-2-S can simulate all extreme precipitation indices (CWD, SDII and PRCPTOT) well compared to the other two models, CMCC-CM2-VHR4 and FGOALS-f3-H. Therefore, the MRI-AGCM3-2-S model will be employed for future projection analysis.

Table 3. Summary of model performance in simulating extreme precipitation indices during boreal winter.

| Model | Indices | | |
|--------|---------|------|---------|
| | CWD | SDII | PRCPTOT |
| CMCC | | | |
| MRI | / | / | / |
| FGOALS | | | |

3.2 Future projections and changes in Malaysia

The higher resolution models can simulate the precipitation increase along the northeast coast of Peninsular Malaysia [11]. Figure 5 shows the future changes in consecutive wet days occurring over the study area under SSP5-8.5 using MRI-AGCM3-2-S model. The whole region shows a significant increase and decrease in wet days in the future. The central and west coasts of Peninsular, the whole of Sabah and north Sarawak show a significant increase in wet days in the future. The highest increment pattern illustrates mostly over North Borneo. However, the east coast and west Sarawak show a significant decrease in the CWD index from 2015 through 2050.

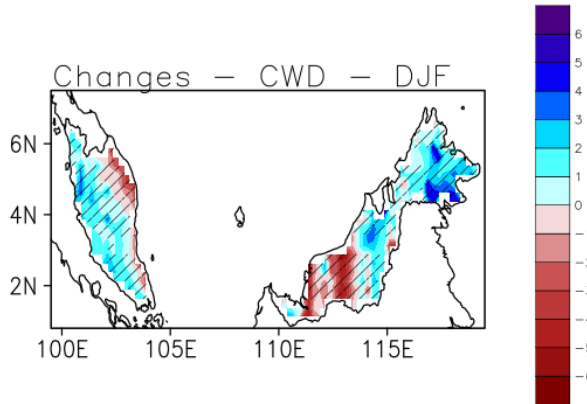


Figure 7. The changes of extreme precipitation index, Consecutive Wet Day (CWD) in Malaysia during boreal winter, DJF. The image is displayed relative to the observation period 1982-2014 under the SSP5-8.5. Areas with hatching represent changes that are significant at the 95% confidence level.

The changes in annual total precipitation during boreal winter are displayed in Figure 6. The west coast of Peninsular and north Borneo pattern shows increases during DJF. There is a significant increase of about 120 mm in annual total precipitation over Southeast North Borneo (at 95% confidence level). However, there are negative value changes over the east coast of the peninsular and most of Sarawak during the near century (2015-2050) under SSP5-8.5. The result is consistent with Ngai, Juneng, Tangang, Chung, Supari, Salimun, Cruz, Ngo-Duc, Phan-Van, Santisirisomboon and Gunawan [12] which shows a decrease in the percentage of PRCPTOT over this region in the future after using the bias correction method.

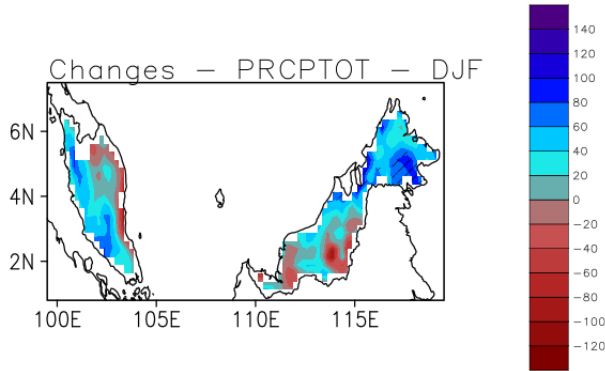


Figure 8. The changes of extreme precipitation index, total annual precipitation (PRCPTOT) in Malaysia during boreal winter, DJF. The image is displayed relative to the observation period 1982-2014 under the SSP5-8.5. Areas with hatching represent changes that are significant at the 95% confidence level.

The changes in simple daily intensity index (SDII) patterns are portrayed in Figure 7. The whole country shows significant changes in the future under SSP5-8.5. On the east coast and the southern part of Peninsular, a few locations including the interior part of Sarawak are facing a decreasing trend of SDII in the future. On the other hand, the west coast of Peninsular and the whole of north Borneo including most areas in Sarawak will have a high trend of SDII in the future under SSP5-8.5. Some areas could face changes up to 2 mm/day as illustrated in Figure 7. This result aligns with Hariadi, van der Schrier, Steeneveld, Sutanto, Sutanudjaja, Ratri, Sopaheluwakan, Klein Tank and Discussions [13] which shows a significant increasing trend over the western part of Peninsular Malaysia and a large part of East Malaysia.

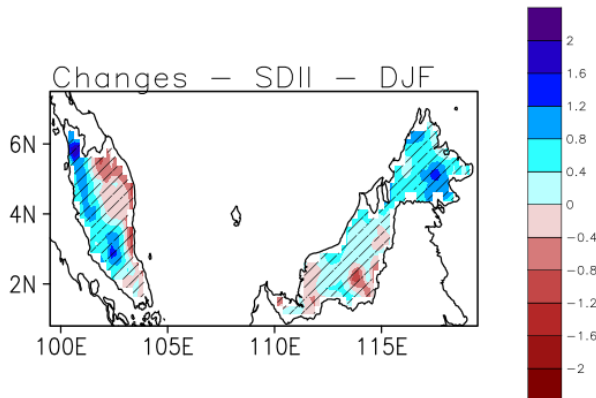


Figure 9. The changes of extreme precipitation index, simple daily intensity index (SDII) in Malaysia during boreal winter, DJF. The image is displayed relative to the observation period 1982-2014 under the SSP5-8.5. Areas with hatching represent significant changes at the 95% confidence level.

All three indices indicate significant future changes under SSP5-8.5 over Malaysia. Index CWD and SDII showed the whole region is expected to face changes in the future. However, the index PRCPTOT showed significant changes only could happen over Southeast North Borneo in the future.

4 Conclusion

The study employs three HighResMIP CMIP6 General Circulation Models (GCMs) to evaluate three extreme precipitation indices over Malaysia during the boreal winter. The MRI model, identified as the most accurate, is selected for future projections from 2015 until 2050 under SSP5-8.5.

Climatologically, Malaysia experiences significant rainfall during the boreal winter due to the influence of the northeast monsoon. All three indices indicate a pronounced intensity of rainfall along the east coast of Peninsular Malaysia and in most areas of Sarawak during this period. All models effectively simulate the three indices, as demonstrated by the Taylor diagram statistical analysis. The MRI model is identified as the most accurate in simulating all three indices and is therefore selected for future projections.

Index CWD and SDII showed significant changes over the whole region which most parts may experience high rainfall and vice versa. For the PRCPTOT index, although regions show both increases and decreases, a significant change is notably observed in the eastern part of Sabah.

Acknowledgements

This research was supported by the Universiti Kebangsaan Malaysia research grant (GUP-2021-042) and LRGS//1/2020/UKM-UKM/01/6/1.

Declaration of Interest Statement

The authors declare no conflict of interest.

References

1. Tangang, F., R. Farzanmanesh, A. Mirzaei, Supari, E. Salimun, A.F. Jamaluddin, and L. Juneng, Characteristics of precipitation extremes in Malaysia associated with El Niño and La Niña events. **37S1**: p. 696-716. (2017)
2. Chang, C.P., Z. Wang, J. McBride, and C.-H. Liu, Annual Cycle of Southeast Asia—Maritime Continent Rainfall and the Asymmetric Monsoon Transition. *Journal of Climate*. **182**: p. 287-301. (2005)
3. Salimun, E., F. Tangang, L. Juneng, S.K. Behera, and W. Yu, Differential impacts of conventional El Niño versus El Niño Modoki on Malaysian rainfall anomaly during winter monsoon. **348**: p. 2763-2774. (2014)
4. Berita, Flooding Caused Overall Losses of RM6.1 Billion Last Year - DOSM, in BERNAMA.COM: Kuala Lumpur. (2022).
5. Haarsma, R.J., M.J. Roberts, P.L. Vidale, C.A. Senior, A. Bellucci, Q. Bao, P. Chang, S. Corti, N.S. Fučkar, V. Guemas, J. von Hardenberg, W. Hazeleger, C. Kodama, T. Koenigk, L.R. Leung, J. Lu, J.J. Luo, J. Mao, M.S. Mizielinski, R. Mizuta, P. Nobre, M. Satoh, E. Scoccimarro, T. Semmler, J. Small, and J.S. von Storch, High Resolution Model Intercomparison Project (HighResMIP v1.0) for CMIP6. *Geosci. Model Dev.* **911**: p. 4185-4208. (2016)
6. Liang-Liang, L., L. Jian, and Y. Ru-Cong, Evaluation of CMIP6 HighResMIP models in simulating precipitation over Central Asia. *Advances in Climate Change Research*. **131**: p. 1-13. (2022)

7. Supari, F. Tangang, L. Juneng, F. Cruz, J.X. Chung, S.T. Ngai, E. Salimun, M.S.F. Mohd, J. Santisirisomboon, P. Singhruck, T. PhanVan, T. Ngo-Duc, G. Narisma, E. Aldrian, D. Gunawan, and A. Sopaheluwakan, Multi-model projections of precipitation extremes in Southeast Asia based on CORDEX-Southeast Asia simulations. *Environmental Research*. **184**: p. 109350. (2020)
8. Alexander, L.V., X. Zhang, T.C. Peterson, J. Caesar, B. Gleason, A.M.G. Klein Tank, M. Haylock, D. Collins, B. Trewin, F. Rahimzadeh, A. Tagipour, K. Rupa Kumar, J. Revadekar, G. Griffiths, L. Vincent, D.B. Stephenson, J. Burn, E. Aguilar, M. Brunet, M. Taylor, M. New, P. Zhai, M. Rusticucci, and J.L. Vazquez-Aguirre, Global observed changes in daily climate extremes of temperature and precipitation. **111D5**. (2006)
9. Alexander, L.V., H.J. Fowler, M. Bador, A. Behrangi, M.G. Donat, R. Dunn, C. Funk, J. Goldie, E. Lewis, M. Rogé, S.I. Seneviratne, and V. Venugopal, On the use of indices to study extreme precipitation on sub-daily and daily timescales. *Environmental Research Letters*. **14**: p. 125008. (2019)
10. Taylor, K.E., Summarizing multiple aspects of model performance in a single diagram. **106D7**: p. 7183-7192. (2001)
11. Liang, J., M.L. Tan, J.L. Catto, M.K. Hawcroft, K.I. Hodges, and J.M.J.C.D. Haywood, Projected near-term changes in monsoon precipitation over Peninsular Malaysia in the HighResMIP multi-model ensembles. p. 1-21. (2022)
12. Ngai, S.T., L. Juneng, F. Tangang, J.X. Chung, S. Supari, E. Salimun, F. Cruz, T. Ngo-Duc, T. Phan-Van, J. Santisirisomboon, and D. Gunawan, Projected mean and extreme precipitation based on bias-corrected simulation outputs of CORDEX Southeast Asia. *Weather and Climate Extremes*. **37**. (2022)
13. Hariadi, M.H., G. van der Schrier, G.-J. Steeneveld, S. Sutanto, E. Sutanudjaja, D.N. Ratri, A. Sopaheluwakan, A.J.H. Klein Tank, and E.S.S. Discussions, A high-resolution perspective of extreme rainfall and river flow under extreme climate change in Southeast Asia. p. 1-29. (2023)